

MECHANISMS OF HAIR CELL TUNING

R. Fettiplace

Department of Physiology, University of Wisconsin, Madison, Wisconsin 53706;
e-mail: fettiplace@physiology.wisc.edu

P. A. Fuchs

Center for Hearing Sciences, Department of Otolaryngology-Head and Neck Surgery,
Johns Hopkins University, Baltimore Maryland, 21205; e-mail: pfuchs@bme.jhu.edu

KEY WORDS: alternative splicing, calcium, calcium-activated potassium channel,
electrical tuning, mechanotransduction

ABSTRACT

Mechanosensory hair cells of the vertebrate inner ear contribute to acoustic tuning through feedback processes involving voltage-gated channels in the basolateral membrane and mechanotransduction channels in the apical hair bundle. The specific number and kinetics of calcium-activated (BK) potassium channels determine the resonant frequency of electrically tuned hair cells. Kinetic variation among BK channels may arise through alternative splicing of *slo* gene mRNA and combination with modulatory β subunits. The number of transduction channels and their rate of adaptation rise with hair cell response frequency along the cochlea's tonotopic axis. Calcium-dependent feedback onto transduction channels may underlie active hair bundle mechanics. The relative contributions of electrical and mechanical feedback to active tuning of hair cells may vary as a function of sound frequency.

INTRODUCTION

The auditory receptor, the cochlea in higher vertebrates, is responsible both for transforming the acoustic stimulus into an electrical signal and for resolving that stimulus into its component frequencies. The relative amplitudes of the different components are then signaled to the brain by activity in VIIIth nerve fibers, each tuned to a narrow frequency band. Acoustic frequency analysis

is an important aspect of sensory perception and helps to shape an animal's behavior. Thus competition and reproduction within most species depend on the spectral analysis of vocal or other acoustic signals. The frequency content of a sound also provides cues for localizing the source. Binaural disparities in sound intensity that are used for localization vary with the size of the animal's head and consequently depend on frequency. Moreover, the external ear reflects and filters sound differentially according to its direction, and thus confers spectral signatures onto defined regions of space (1, 2). Acoustic frequency analysis is therefore fundamental to sound localization, communication, and the detection of predators and prey.

Extrinsic Versus Intrinsic Tuning

The importance of frequency analysis in inner ear function is emphasized by the assortment of mechanisms that have evolved to implement this task in species ranging from insects to humans (3). Among this variety, two general design principles are found: an extrinsic mechanism in which the stimulus is filtered prior to hair cell transduction, and one where the filtering is intrinsic to the hair cell. The mammalian cochlea exemplifies an acoustic detector in which filtering is performed at least partly by the accessory structures in which the neural elements are embedded. Owing to the graded mechanical properties of the basilar membrane, different frequencies displace it maximally in different places, which results in a tonotopic map of vibration frequency (4). Thus a small range of frequencies is imparted to each inner hair cell, which transduces the narrow-band stimulus, thereby generating tuned receptor potentials. This filter is extrinsic to the hair cell, in analogy to that of the Pacinian corpuscle, where rapid adaptation arises largely from the mechanical properties of the accessory bulb that encapsulates the sensory ending.

In contrast, in the auditory papilla of the turtle, the filter is wholly intrinsic to the hair cell. Here the mechanics of the basilar membrane impart meager tuning, and transduction current is driven into the hair cell nearly equally by a broad range of stimulus frequencies. The amplitude of the receptor potential is then modulated by voltage-dependent ionic conductances that confer a property of electrical tuning onto the hair cells. An analogy may be drawn with color perception in the visual system, where different wavelengths in the light are detected by red, green, and blue cone photoreceptors, each maximally sensitive over a different spectral range. The resonant frequencies of turtle hair cells vary systematically along the length of the basilar papilla, resulting in a tonotopic organization similar to that arising from mechanical tuning in the mammal. The extrinsic and intrinsic acoustic tuning processes may not be totally independent because interactions between the two can occur by mechanical feedback from the hair cells, as is discussed below. Such feedback is thought to be involved

in augmenting the tuning of the basilar membrane in the mammalian cochlea (5).

This review focuses on those features intrinsic to the hair cell that participate in their tuning and mechanosensitivity. The ion channels that comprise the mechanism of electrical tuning are discussed in the section ELECTRICAL TUNING. In the section MECHANICAL TUNING other hair cell properties that also vary along the tonotopic axis are described, with special emphasis on mechanical tuning by the transduction apparatus.

ELECTRICAL TUNING

Hair Cell Tuning in the Turtle Basilar Papilla

The low-frequency hearing (30–600 Hz) of the red-eared turtle *Trachemys scripta elegans* is served by a receptive epithelium, the basilar papilla, which contains roughly 1000 hair cells in a strip approximately 1 mm in length (6, 7). Direct measurements of basilar membrane motion using laser interferometry revealed no position-dependent mechanical tuning (8). Nonetheless, recordings from hair cells and afferent fibers in a semi-intact preparation showed sharp tuning and sensitivity, with an orderly sequence of best frequencies mapped along the basilar papilla (9, 10). The combined tuning curves of all afferent fibers possessed a minimum threshold and total frequency range matching the turtle's behavioral audiogram (11).

Intracellular recording from turtle hair cells showed that they were not passive reporters of mechanical input. Current pulses injected into hair cells caused a damped oscillation of the membrane potential (Figure 1) with frequency and decay rate similar to those elicited by an acoustic transient (click) to that same cell (12). This behavior, termed electrical resonance, was attributed to the voltage-dependent activation of a membrane K^+ conductance. The optimal frequencies and bandwidths of tuning for both the electrical and acoustic stimuli were essentially identical in each of a population of hair cells spanning much of the turtle's audible range. Therefore in the turtle there is little or no filtering of the acoustic stimulus prior to mechano-electrical transduction (13).

BK Calcium-Activated Potassium Channels Tune Hair Cells

Electrical tuning has also been observed in hair cells of fish, frogs, alligators, and chicks (14–19). Voltage-clamp recording from frog saccular hair cells suggest that the interaction between a voltage-gated Ca^{2+} current and a K^+ current flowing through large conductance Ca^{2+} -activated K^+ (BK) channels produces the oscillatory voltage responses (17, 20, 21). The basis of the electrical resonance can be explained by considering the sequence of events following a current step: (a) depolarization opens voltage-gated Ca^{2+} channels, promoting

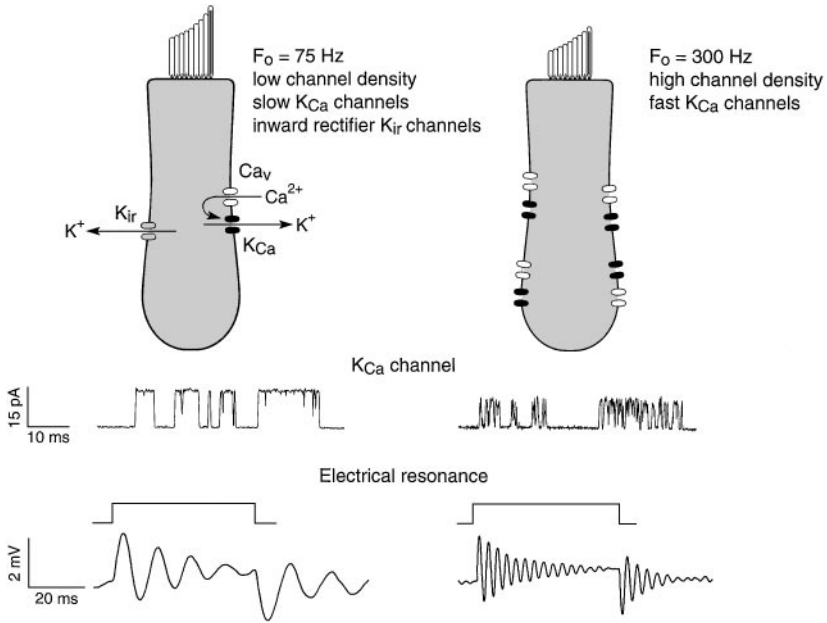


Figure 1 Schematic drawing of two hair cells from the turtle basilar papilla, with resonant frequencies (F_0) of 75 and 300 Hz. The low-frequency cell has a longer hair bundle, and a low density of Ca^{2+} and Ca^{2+} -activated K^+ (K_{Ca}) channel complexes. The number of channel complexes increases with (F_0). Beneath each cell are shown representative K_{Ca} (BK) single-channel records and ringing voltage responses to extrinsic current steps for cells tuned approximately to these two frequencies. The timing of the extrinsic current is shown above the voltage records. The single-channel records and the voltage ringing were from different sets of experiments (22, 23).

a rise in internal Ca^{2+} that activates BK channels; (b) the large outward K^+ current hyperpolarizes the membrane, closing the Ca^{2+} channels, which leads to the first cycle of the oscillation; (c) as the cell hyperpolarizes and intracellular Ca^{2+} transients dissipate, the BK channels partially close, but due to the continued extrinsic current, the membrane swings positive to initiate another cycle of Ca^{2+} influx. Since the BK channels are already partly activated, a smaller fraction of K^+ current is recruited on the second cycle, which will have a smaller amplitude than the first. Because the K^+ equilibrium potential (-80 mV) is negative to the resting potential (-50 mV), the BK channels behave as part of a negative feedback loop, but the time course of their activation delays the feedback and hence generates damped oscillatory responses.

Such negative feedback also produces sharp tuning for sinusoidal stimuli, and the frequency at which the cell is maximally sensitive, the resonant frequency, should be influenced by the size and speed of the feedback. The factors

determining the resonant frequency were studied experimentally in turtle hair cells tuned to a range of frequencies (22). As in the frog, the electrical resonance was generated in most cells by the interaction of voltage-gated Ca^{2+} channels and large-conductance, Ca^{2+} -activated K^+ (BK) channels. A cell's resonant frequency was correlated with the characteristics of its BK channels, a higher frequency arising from an increase in the number of channels and, more importantly, from faster channel kinetics.

Analysis of single BK channels in membrane patches excised from turtle hair cells (23) demonstrated that the kinetic differences were intrinsic to the BK channel (Figure 1). The mean open time and relaxation time constant of ensemble-averaged currents at a fixed intracellular Ca^{2+} varied approximately 30-fold (0.4–13 ms) among BK channels from hair cells tuned to different frequencies. The Ca^{2+} sensitivity and unitary conductance in contrast were indistinguishable in all channels. A kinetic scheme of BK gating based on measurements from single channels, when combined with voltage-gated Ca^{2+} influx and accumulation, quantitatively accounts for electrical tuning over a frequency range from 40 to 600 Hz (24). For a subset of hair cells with resonant frequencies less than 40 Hz, tuning is achieved by replacing the BK channels with other voltage-gated K^+ channels.

Voltage-Gated Ca^{2+} Channels

Voltage-gated Ca^{2+} channels have been characterized in hair cells of several different species (20, 22, 25–29). In all cases, these channels activate with a time constant of less than 0.5 ms at -50 mV, do not inactivate, and deactivate very rapidly upon repolarization. The Ca^{2+} current is reduced by dihydropyridine antagonists, suggesting an L-type channel, but the hair cell Ca^{2+} channels differ from L-type channels in other cell types by more rapid gating kinetics, a more negative activation range, and lower sensitivity to dihydropyridine antagonists (29). The full-length sequence of an α_{1D} calcium channel has been cloned from the basilar papilla of the chick and is the most likely candidate for the hair cell's channel (30).

BK channels require a relatively high Ca^{2+} concentration to open ($K_{1/2} \sim 12 \mu\text{M}$ at -50 mV) and so must be located in close proximity to the voltage-gated Ca^{2+} channels (24, 27). The co-localization of Ca^{2+} and BK channels, and high concentration of mobile Ca^{2+} buffer, ensure that excursions in Ca^{2+} concentration at the internal face of the BK channel follow with little delay the gating of the Ca^{2+} channels. Thus the kinetics of BK gating become the rate-limiting step in determining the frequency of electrical tuning. In the turtle, a hair cell's complement of voltage-gated Ca^{2+} channels increases with its resonant frequency, but the numbers of Ca^{2+} and BK channels maintain a fixed ratio of about 2:1 in all cells (31). This suggests that the two channel types

are coregulated, which could be achieved by insertion into the membrane of channel complexes composed of two Ca^{2+} channels linked to each BK channel.

BK Channels—Alternatively Spliced slo Gene Products

To understand the regulation of the electrical tuning it is important to know the origin of the kinetic variation of the BK channels. There is currently no evidence that the channel kinetics are controlled by an intracellular modulator, and the simplest alternative hypothesis is that the variation arises from differential expression of distinct kinetic isoforms of the channel. What is the minimum number of channel variants that can account for the frequency range? Modeling of electrical tuning in the turtle indicated that five species of BK channel with different kinetics and overlapping distribution were sufficient to cover the animal's auditory range (40–600 Hz) (32). Extension of this model to the chick basilar papilla, which has a greater frequency range (150–4000 Hz) and operates at higher temperature, required a minimum of nine species of BK channel.

The BK channels that support electrical tuning in hair cells are most likely a product of a single *slo* gene originally described in *Drosophila* (33, 34) and subsequently found in mammals (35–37). A full-length homologue was cloned from a chick cochlear cDNA library and shown to encode the α -subunit of the BK channel when expressed in HEK 293 cells (38). The coding region of cSlo1 predicts an 1137 amino acid protein that is 94% identical to a human brain *slo* (*hbr1*) (36) and may correspond to a minimal length transcript (the fewest exons). The cSlo1 channels had a conductance of 224 pS in symmetrical K^+ solutions, were blocked by external charbydotoxin or iberiotoxin and by low concentrations of tetraethylammonium ions, and were sensitive to intracellular Ca^{2+} , with half-activation at 0 mV by approximately 20 μM Ca^{2+} . RT-PCR from the basilar papilla or from single isolated hair cells confirmed the expression of this cDNA in hair cells. A homologous minimal length cDNA has also been identified in turtle basilar papilla (39) and described in other studies on chick (40, 41).

The *slo* gene encodes a channel protein predicted to contain seven transmembrane segments, an extracellular N terminus (42), a pore region with homology to Shaker-type K^+ channels, and a long intracellular C-terminal segment that includes part of the Ca^{2+} -binding site (43). Multiple alternative exons are found at several splice sites within the *Drosophila* and mammalian transcripts. Some splice variants have altered gating kinetics (44, 45), suggesting that alternative splicing of *slo* mRNA could provide the functional heterogeneity found in hair cell BK channels. Indeed, hair cell *slo* transcripts are alternatively spliced (Figure 2). Eight potential splice sites have been identified and 15 alternative exons have been described to date (38–41).

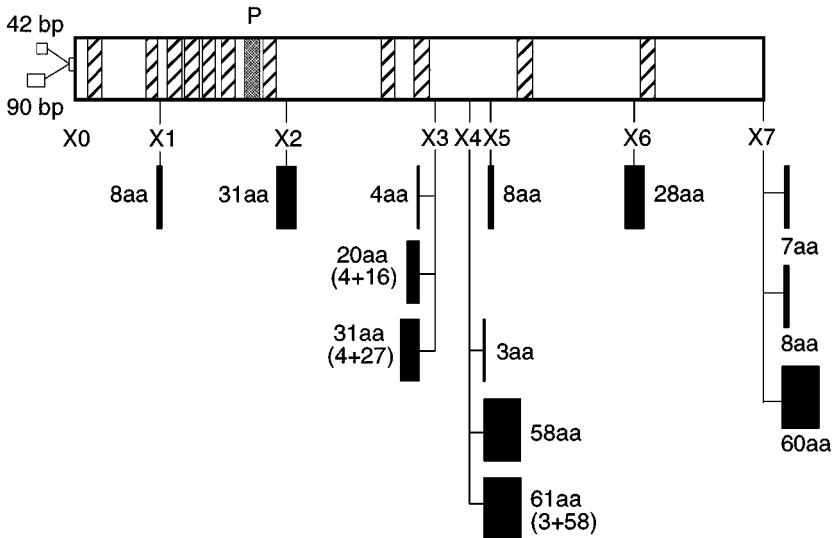


Figure 2 Schematic diagram of the cochlear Slo channel α -subunit open reading frame (~ 1150 amino acids in length), carboxy terminus to the right. *Hatched boxes* are putative amphipathic or transmembrane domains (S0–S10) based on data of Meera et al (42), and the *shaded area* is the pore (P). Eight splice sites, X0–X7, have been identified. Two 5' sequences have been identified (38, 41). Both contain additional in-frame ATGs, but these are not necessary for producing a functional channel (36, 148) and may therefore be located in the untranslated region. At X7, three exons give rise to different carboxy termini of 7, 8, and 60 amino-acids (aa) (38–41; note a single residue difference in the 8 aa exon among these reports). X1–X6 may have no insert or contain a single exon or concatenated exons, the amino-acid sizes of which are noted below each site. X1, which is novel among all vertebrate and invertebrate BK transcripts, may contain an 8 aa insert (41); X2 may contain a 31 aa insert (40). X3 may contain a 4 aa (39–41), a 20 aa (41), or a 31 aa (39) insert. X4 may contain a 3 aa (39, 40), a 58 aa (41), or a 61 aa (39) insert. The 58 aa insert is reported as 59 but includes a modified 5' flanking amino acid. X5 may contain an 8 aa insert (41) and X6 a 28 aa insert (40, 41; note the reported sequences differ by a single residue).

Distribution and Function of Alternatively-Spliced slo Variants in the Cochlea

Hair cells in both the avian and turtle basilar papillae are mapped tonotopically, with the cell's resonant frequency increasing monotonically along the length of the sensory epithelium. If alternative splicing underlies variations in hair cell tuning, then expression of BK splice variants should be spatially localized within the epithelium. In situ PCR showed that expression of the exon X3 = 4 was restricted to the middle third of the basilar papilla of the embryonic chick and was absent from the basal (high-frequency) tip of the post-hatch cochlea (41). Quantitative PCR from microdissected quadrants of the basilar papilla

indicated that exon X2 = 31 was excluded from the low-frequency quarter of the cochlea (40). In this latter study, X3 = 4 appeared equally in all quadrants, in contrast to the result with in situ PCR (41). X4 = 0 was preferentially expressed in quadrants 2 and 3 from the apex. The distributions of two carboxy termini were found to differ, with X7 = 8 occurring at higher levels in quadrants 3 and 4.

In the turtle's basilar papilla, only a restricted subset of sites (X3 and X4 in Figure 2) appear to be alternatively spliced, and only the long (X7 = 60) form of the carboxy terminus is present. It was thus possible to determine some of the exon combinations occurring naturally (39). The combinations, specified by the amino acid insert sizes in X3 and X4, respectively, include 0-0, 4-0, 4-3, 4-61 and 31-3. The spatial distribution of the most prevalent isoforms was studied by RT-PCR on groups of hair cells isolated from different regions. The combinations 4-3 and 31-3 were absent from the highest frequency quadrant. It is worth noting that in both turtle and chick, the distributions observed are quite broad, involving 50% of the papilla or more. However, the amplification techniques do not as yet allow a conclusion about a gradient in the level of a particular mRNA transcript in these broad regions. Moreover, the occurrence of the message does not necessarily reflect the extent of channel incorporation into the membrane. It will be important to verify (by techniques such as antibody labeling) that the protein isoforms encoded by the different transcripts are indeed expressed in the hair cell plasma membrane.

The functional effects of alternative splicing are beginning to be explored. Two carboxy-terminal splice variants, X7 = 8 and X7 = 60 (homologous to the termini originally described in human and mouse Slo, respectively), produced functionally identical channels when expressed in HEK cells or *Xenopus* oocytes (46). Splice site X4 in turtle includes a 61 amino acid exon that is related to the 59 or 61 amino acid exon described in adrenal chromaffin cells (45, 47). In studies of chick Slo variants, addition of X4 = 61 to the cSlo backbone caused a two- to threefold slowing of deactivation kinetics, as well as a 25 mV negative shift in the half-activation voltage (48). While studies of individual added exons can be instructive, ultimately it will be necessary to characterize and test those combinations of exons that predominate in hair cells if the native channels are to be reconstituted. In the chick, the occurrence of alternative splicing at seven sites within the coding region implies that a potentially large number of combinations may exist, which makes the task of assigning functional consequences to different variants daunting.

However, the restriction of splicing in the turtle channel to just two sites, X3 and X4, suggests that one or both of these sites is crucial for determining the channel properties, including its Ca²⁺ sensitivity and kinetics. Expression of the different turtle α -subunit variants in *Xenopus* oocytes has confirmed this

notion (49). In order to match the performance of native channels, reconstitution will most likely require accessory β -subunits that are known to influence the channel's behavior (50). Preliminary results indicate that coexpression of hair cell α -subunit with a β -subunit both increased the channel's Ca^{2+} sensitivity and markedly slowed its kinetics (49, 51). Thus in theory a range of channel kinetics might be achieved by differential expression of different splice variants of the α -subunit in conjunction with an expression gradient of a β -subunit.

Hair Cell Tuning with Other K^+ Channels

As in turtles and frogs, electrical tuning in alligator and chick hair cells arises from the interaction of voltage-gated Ca^{2+} and Ca^{2+} -activated K^+ currents (18, 19). However the use of BK channels is confined to frequencies above 100 Hz, and at lower frequencies the outward current of hair cells in these species is dominated instead by a slowly activating calcium-independent, delayed-rectifier K^+ current (52). In addition, these cells have an inward rectifier K^+ current that makes a contribution to membrane conductance at potentials negative to -40 mV. Such cells have more negative resting membrane potentials and generate low frequency (<30 Hz) oscillations or slowly repetitive calcium action potentials. In alligator hair cells, a TTX-sensitive sodium current can assist with spiking (53).

Voltage-gated K^+ channels have also been shown to be involved in tuning of turtle auditory hair cells (54, 55). Slowly activating voltage-dependent K^+ currents and inward rectifier currents are responsible for tuning to the lowest frequencies (10–40 Hz) in apical hair cells. Use of a delayed rectifier may reflect the need to slow the activation kinetics of the K^+ current below that obtainable with a pure BK current. Inward rectifier K^+ currents also serve to augment the sharpness of tuning in cells containing BK channels tuned to frequencies less than 200 Hz (24, 55). The utilization of delayed rectifier and inward rectifier K^+ channels by low-frequency hair cells implies that expression of these types of K^+ channel may be confined to the apical region of the cochlea. RT-PCR was used to demonstrate that the inward rectifier cIRK1 (56) and a chick homologue of the Shaw K_v family, c $\text{K}_v3.1$ [a putative delayed rectifier (40)], were preferentially expressed in segments microdissected from the apical half of the chick's basilar papilla.

Determinants of Ion Channel Expression in Hair Cells

The expression of ion channels may be related to the synaptic organization of hair cells. It has been suggested that voltage-gated Ca^{2+} channels and BK channels cluster preferentially at transmitter release sites in frog saccular hair cells (27, 57), as observed at the neuromuscular junction (58). The relationship between Ca^{2+} channel expression and release site formation was examined in

chick hair cells, among which afferent innervation density varies systematically by cochlear position (59). Release site size is greater in more basally located hair cells, but release site number falls across the cochlear width (see color insert C1, Figure 3, at back of volume). Ca^{2+} channel number was found to correlate with each hair cell's total release area—a product of release site number and size. A tonotopic gradient of Ca^{2+} channels in turtle hair cells also may be related to variations in presynaptic structure, with the highest frequency hair cells having the largest calcium currents (22, 31) and the greatest number of release sites (60).

Gradients of innervation and ion channel expression are observed across, as well as along, the sensory epithelium. The differential innervation by afferent and efferent neurons across the width of the chick's basilar papilla (61) corresponds to cell-specific expression of various voltage-gated potassium channels (62). Hair cells with predominately efferent innervation have rapidly inactivating A-type K^+ currents, whereas hair cells innervated by afferent neurons possess the delayed rectifier and inward rectifier currents described above. These pre- and postsynaptic K^+ currents are reminiscent of the synaptic distributions of K_v subtypes described in mammalian brain (63). It will be of interest to examine the distribution of ion channels in hair cells that have developed with altered innervation in vitro (64) or following denervation (65).

Studies of hair cell development may offer additional insights into potential regulatory mechanisms. BK-type whole-cell currents are first elicited from chick cochlear hair cells at about embryonic day 18 (66), coincident with a late stage of functional maturation of the cochlea (67, 68). In contrast, Ca^{2+} channels and delayed rectifier K^+ channels appear as many as 7 days earlier, and together support calcium spiking in the embryonic hair cell. Even at embryonic day 10, chick hair cells express different classes of voltage-gated K^+ channels depending on their cochlear position (69). Thus developmental schedules, and presumably the underlying regulatory mechanisms, are channel specific during hair cell differentiation. One might imagine that spontaneous (or driven) activity and associated Ca^{2+} flux in embryonic hair cells provides some instruction for the later expression of BK channels, as occurs during the developmental acquisition of K^+ channels by embryonic *Xenopus* neurons (70).

MECHANICAL TUNING

Passive Resonance of the Hair Bundle

The auditory signal can be filtered during the process of mechanotransduction in the hair bundle, as well as by the subsequent activity of voltage-dependent channels in the basolateral membrane. Acoustic stimuli give rise to vibrations of the basilar membrane, which are translated into a to-and-fro motion of the hair

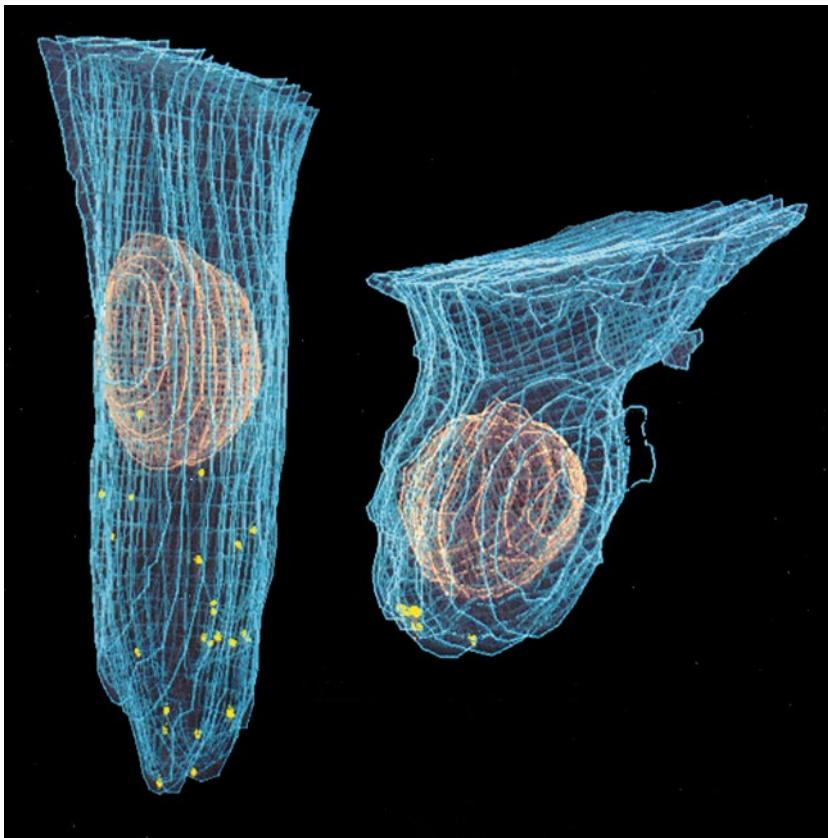


Figure 3 Three-dimensional reconstructions of mechanosensory hair cells from the cochlea of a chick, derived from serial electron micrographs. Presynaptic dense bodies found at sites of transmitter release are shown in *yellow*. Tall (inner) hair cells (*left*) contact the majority of afferent neurites and have more numerous release sites and voltage-gated calcium channels than do short (outer) hair cells (*right*) (59). The nuclei (*brown*) are approximately 4 μm in diameter. Image provided by RL Michaels, Univ. Colorado Health Sciences Center.

bundle, an array of 50 or more stereocilia that forms the hair cell's mechanosensory organelle. The bundle is wedge-shaped and the heights of sequential ranks of stereocilia increase from one side of the bundle to the other, thus defining an axis of symmetry along which the bundle normally rotates. Relative motion of adjacent stereocilia is detected by mechanotransducer channels located at the stereociliary tips (71–73). The channels are thought to be gated by force delivered through extracellular tip-links connecting the top of one stereocilium to the side wall of its taller neighbor (74, 75).

In most vertebrates, the structure of the hair bundle varies along the cochlea's tonotopic axis, with a decrease in the height of the stereocilia toward the high-frequency end (76–78). Reduction in bundle height is often accompanied by an increase in the number of stereocilia per bundle (7, 79, 80). The chick basilar papilla is a well-documented example, where bundle height decreases from 6 to 1.5 μm , and the number of stereocilia increases from 50 to 300 from the low- to high-frequency end (79). Direct manipulation of the bundle has shown that the stereocilia are rigid and move as a concerted array, pivoting about their base with no flexure along their length (81–83). At first glance, therefore, the hair bundles should behave as mechanical resonators like the arm of a tuning fork, with the resonant frequency being a function of the bundle's stiffness and mass. The number of stereocilia per hair cell, the links interconnecting them, and the maximum height of the bundle all contribute to the hair bundle stiffness (84). In a simple analysis, if the bundle contains stereocilia of mean length L , each with a rotational stiffness K_B , the free bundle's undamped resonant frequency F_B is given by

$$F_B = k K_B^{0.5} L^{-1.5}, \quad 1.$$

where k is a constant. The resonant frequency is inversely proportional to the stereociliary length to the three halves power predicting that shorter bundles should resonate at a higher frequency (85). In this treatment, the bundle stiffness is assumed to be constant, but this is likely to be an oversimplification owing to the active bundle movements discussed below.

In the majority of species, passive resonance of the hair bundle probably contributes little to cochlear frequency selectivity. The resonant frequencies estimated from Equation 1 are inappropriately high (82, 86), and the predicted resonance is likely to be over-damped. A further limitation is that the bundles do not vibrate independently but are usually coupled laterally and longitudinally via attachments to an acellular tectorial membrane that carpets the entire papillar surface. Exceptions to this rule are found in several lizard species (87), where the basilar papilla is subdivided into regions with distinct morphologies. In one region, the hair bundles are connected to a continuous tectorial membrane in an arrangement common to most other vertebrates. In a second region,

either the tectorial membrane is absent or there are a series of specialized tectorial structures, the sallets, each attached to only a small cohort of hair bundles. In the alligator lizard *Gerrhonotus multicarinatus*, cells in the high-frequency region of the papilla possess very long, free-standing bundles with no connection to a tectorial membrane (76). Both theoretical analysis (85, 88) and direct experimental observations (89, 90) indicate that the bundle resonance provides some frequency tuning. The bundle heights decrease from 30 to 12 μm in conjunction with an increase in characteristic frequency from 1 to 4 kHz, a correlation that is in good agreement with Equation 1 (85).

A sharply tuned passive resonance can also be achieved by employing shorter stereocilia but increasing the mass loading of the bundles with tectorial sallets coupled to a row of about ten hair bundles. This organization has been described and modeled in both the bobtail lizard *Tiliqua rugosa* (91) and the Tokay gecko *Gekko gecko* (92). For example, in the gecko, a gradient in hair bundle height from 16 to 5 μm (80) combined with the mass of tectorial sallets produces a passive resonance predicted to tune the hair cells to frequencies from 1 to 5 kHz. Both the free-standing bundles and sallet-loaded bundles are specializations that may have evolved to expand the high-frequency range of the hearing organ up to about 5 kHz. For these lizard species, there is an additional portion of the basilar papilla possessing a conventional tectorial canopy and receptor cells tuned to lower frequencies; in the gecko, hair cells in this portion probably employ an electrical tuning mechanism to encode frequencies from 0.15 to 0.8 kHz. (93).

There is at most a 5-fold variation in bundle height in a given cochlea, which (from Equation 1) yields only a 11-fold change in the passive resonant frequency. Without assuming variations in other factors, such as stereociliary rotational stiffness or tectorial mass loading, changes in bundle height are inadequate to explain the wide frequency range of most cochleae. What role then does the ubiquitous tonotopic variation in bundle structure play? One simple consequence of reducing bundle height and increasing stereociliary number at high frequencies will be to enhance the sensitivity of transduction. A given motion of the tectorial membrane will cause shorter bundles to undergo a larger angular rotation. When this factor is combined with the larger transducer current (from increases in numbers of both stereocilia and transducer channels per stereocilium; 94), it can, in theory, generate in the turtle a 10-fold increase in the sensitivity of transduction at high frequencies.

Transducer Currents and Adaptation

To examine other tuning processes intrinsic to the hair bundle, it is first necessary to document the properties of the transduction mechanism. Performance of the transducer channels has been assessed either by measuring extracellular

microphonic currents (95, 96) or by recording transducer currents in isolated voltage-clamped hair cells (97–100) during manipulation of the hair bundle. Both methods have demonstrated that the channels respond maximally for bundle rotations of $\pm 5^\circ$ (equivalent to $\pm 0.5 \mu\text{m}$ deflection at the tip of a $6 \mu\text{m}$ bundle). The channels activate with time constants on the order of 0.1 ms at room temperature (95, 99), but in response to a maintained stimulus, they close again because of an adaptation process that resets the bundle's operating range. Depending on the measurement conditions and preparation, the adaptation time constant can range from 0.3 ms to more than 30 ms (94–96, 99, 101). Transduction in solitary hair cells is often compromised by mechanical damage incurred during the isolation procedure. Such damage can be minimized by patch-clamping hair cells in an intact cochlear epithelium (102), where larger currents and faster adaptation are observed. When this approach was applied to the turtle cochlea, the properties of the transducer current were found to vary with hair cell position along the tonotopic axis (94). In progressing from the low-frequency to the high-frequency end of the cochlea, the maximum transducer current increased more than fivefold and the time constant of adaptation decreased nearly tenfold. The turtle basilar papilla exhibits trends in hair bundle morphology similar to those described elsewhere (7), with a halving in bundle height (10 to $5 \mu\text{m}$) and an approximate doubling in stereociliary number (50 to 90) in high-frequency hair cells compared with low-frequency hair cells. Variation in the number of stereocilia is insufficient alone to explain the gradient in the transducer current, and a change in the number of transducer channels per stereocilium must also be assumed (94). An increase in number of transducer channels per stereocilium will result in a larger Ca^{2+} influx that may partly account for the acceleration of adaptation in high frequency hair cells (see below).

The systematic variation in adaptation time constant along the cochlea (Figure 4) from 4 ms to less than 0.5 ms suggests that adaptation contributes to hair cell frequency selectivity. Dissection of the hair cell's acoustic tuning curve in the turtle cochlea (12) revealed that, apart from the major component endowed by the electrical resonance, there was a residual low-pass filter attributed to the middle ear mechanics and a single-pole high-pass filter of unknown origin. The high-pass filter varied from 29 to 350 Hz and was roughly scaled with the hair cell's characteristic frequency. A similar high-pass filter range was inferred from tuning curves during efferent stimulation that nullifies the electrical resonance (103). A variation in the time constant of transducer adaptation could account for this filter (94). The smooth curve in Figure 4 was calculated on the assumption that transducer adaptation contributes a high-pass filter with a 3 dB corner frequency of 0.7 of the cell's characteristic frequency. It should be emphasized that the absolute values of the time constant will vary

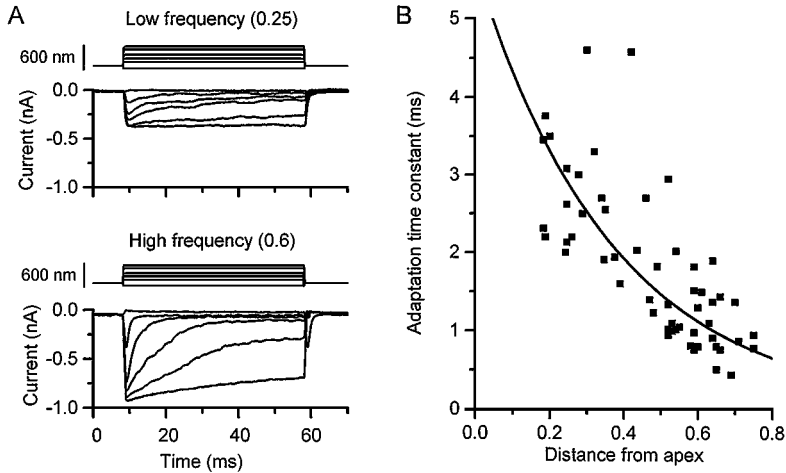


Figure 4 (a) Families of transducer currents from two hair cells near the low-frequency end (*top*) and high-frequency end of the turtle basilar papilla (*bottom*). Numbers in parentheses denote hair cell position as the fractional distance, d (0 to 1), from the low-frequency apical end. Note the currents in the high-frequency cell are larger and, for small stimuli, adapt more rapidly. Traces above current records represent deflections of the hair bundle. Holding potential -90 mV, intracellular Ca^{2+} buffer, 1 mM BAPTA. (b) Adaptation time constants, τ_a , of 53 cells against fractional distance of a cell from the low-frequency (apical) end of cochlea. Smooth curve was calculated on the assumption that adaptation contributes a high-pass filter with a 3 dB corner frequency of 0.7 of the cell's resonant frequency (F_0). The time constant of adaptation, τ_a , in milliseconds, is related to F_0 and, assuming an exponential frequency map (32), to d , the fractional distance along the cochlea from the low-frequency end by $\tau_a = 1000/1.4 \pi F_0 = 5.68 \exp(d/0.37)$.

to some extent depending on the external Ca^{2+} concentration and the intracellular Ca^{2+} buffer (94, 104), but nevertheless, the relative range is approximately correct.

The mechanism of transducer adaptation is still incompletely understood, but it is generally agreed to be regulated by changes in stereociliary Ca^{2+} concentration following influx of the divalent ion through open transducer channels (94, 98, 99, 105). The change in Ca^{2+} then resets the range of displacements detected by the channel. One mechanism by which this resetting might be accomplished entails a myosin motor connected to both the transducer channel and the actin cytoskeleton of the stereocilium (106). Ca^{2+} influx is postulated to inhibit the actomyosin interaction, causing the channel to slip down the side-wall of the stereocilium and thereby reduce the extension in the tip-link. Circumstantial evidence in support of this motor hypothesis includes the demonstration that myosin 1β is present near the tips of the stereocilia in frog

sacculus hair cells (107). In addition, adaptation is blocked by ADP β S (108) and by various phosphate analogs (109) that interfere with myosin ATPases. However, it should be stressed that all such agents also inhibit the Ca ATPases responsible for Ca²⁺ extrusion from hair cells (110, 111) and thus affect the stereociliary Ca²⁺. Whether such an actomyosin interaction is rapid enough to account for the fastest adaptation time constants observed in turtle hair cells (<0.5 ms) is also presently unclear, and a more direct action of Ca²⁺ on the transducer channel may be required. Nevertheless, the scheme whereby the transducer channels are under negative feedback control is widely accepted.

Feedback Control and Tuning of the Transducer Current

Feedback control of the transducer channels arises because the transducer current is a function of the difference between the external stimulus and an internal set position for the channel determined by the level of intracellular free Ca²⁺. As the transducer channels open during bundle deflection, Ca²⁺ enters the stereocilia and triggers adaptation, which acts to close the channels. As with other negative feedback systems, the transducer current may be tuned under certain conditions. Such tuning has been observed in turtle hair cells and is manifested as an under-damped oscillation of the voltage-clamped transducer current for small positive displacements. Resonant frequencies of 58 to 230 Hz have been measured (104). Whether adaptation displays an over-damped exponential decay or an under-damped oscillation depends on a variety of experimental factors including the magnitude of the transducer current, the intracellular Ca²⁺ buffering, and the external Ca²⁺ concentration. The resonance will occur at a frequency related to the rate of opening of the transducer channels and the speed of the adaptive feedback. It should be noted that this resonance in the transducer current does not require an active motor to produce the feedback. However, if the change in the channel's set point is achieved by a motor (101), then a mechanical output may be generated.

A useful analogy can be drawn between active transducer feedback and the electrical resonance. The passive electrical properties of the hair cell membrane, resulting from a leak resistance and a membrane capacitance, provide only a low-pass filter, but the addition of negative feedback by voltage-dependent activation of K⁺ channels can generate a sharply tuned resonance. In a similar manner, a displacement-sensitive feedback on the transducer channels could generate a sharply tuned transducer current.

Active Hair Bundle Movements

Active movements of the hair bundles have been described in a number of lower vertebrate preparations. Such movements were manifested as spontaneous fluctuations in bundle position (82, 112–114), nonlinear responses to

force steps (82, 112, 115), and motion evoked by intracellular current injection (82, 98, 101, 113, 116). The motion is regarded as active because its amplitude, ranging from 5 to 100 nm, exceeds that expected for the Brownian motion of a passive resonator (82). Whether the assorted observations reflect a single underlying mechanism is unclear.

In addressing the mechanism of the bundle motor, the experimental phenomenon may be categorized according to the speed of the active process. Some movements, epitomized by the responses to current injection reported by Assad & Corey (101), take place over 100 ms or more. This time course is correlated with that of transducer adaptation in bullfrog saccular hair cells and appears sufficiently slow to be mediated by the myosin motor detailed above. In contrast, some active movements occur on a millisecond time scale (82, 112) and have been referred to as rapid twitches (115) to distinguish them from the slower manifestations of adaptation. The faster motion may underlie the fast adaptation rates recently described in turtle hair cells (94).

A unifying hypothesis is that there are two Ca^{2+} -dependent processes to channel regulation, both of which could potentially involve myosin. In the slower component, myosin ratchets up and down the core of the stereocilium, detaching from and reattaching to the actin cytoskeleton and ferrying the channel with it in order to adjust the tension on the tip-links (106). In the faster component, there is a modulation of the transducer channel (99, 100) mediated either directly by an interaction of Ca^{2+} with the channel protein, or indirectly via myosin, which merely rocks back and forth without detachment from the actin cytoskeleton (106). Evidence that the hair cells are capable of creating a significant active force-output, even in lower vertebrates, is provided by the observations of spontaneous otoacoustic emissions. An especially compelling example was recently reported in the lizard *Anolis sagrei* (117), where the otoacoustic emissions were related to the number of hair cell generators in the high-frequency portion of the basilar papilla. In some other lizards and in some birds, the spontaneous otoacoustic emissions also appear to be confined to a frequency range corresponding to the high-frequency region of the papilla (118).

The role of active mechanical feedback in the tuning of individual hair cells is still poorly defined and remains an area for future exploration. How and where might it be employed? The obvious site for such a mechanism would be at high frequencies, where electrical tuning may have been abandoned because of the inordinately high densities and fast kinetics of K^+ channels required to achieve tuning at such frequencies (24). In lower vertebrates, electrical tuning seems adequate to explain auditory frequency selectivity at frequencies below 1 kHz. Avian cochleae utilize electrical resonance (19) and contain two types of hair cell (119), each arranged in multiple rows: a columnar inner hair cell (the tall cells) along the edge of the basilar membrane that receives the majority of the

afferent innervation, and a flattened outer hair cell (the short hair cell) situated toward the center of the basilar membrane and innervated predominantly by efferent neurons (see color insert C1, Figure 3, at back of volume). This arrangement is striking in that it resembles the mammalian organization.

Although the role of the avian short outer hair cells is not established, it is tempting to suppose that, by analogy with their mammalian counterparts, they perform a motor function supplying tuned energy into the vibration of the cochlear partition, which itself displays some mechanical tuning (120). Because the cell bodies of the short hair cells are anchored to supporting cells in the basilar papilla, they can deliver force only via hair bundle motion. This movement in the short hair cells would be transmitted to the tall hair cells on the neural limbus via the overlying tectorial membrane. The proportion of short outer hair cells increases toward the basal end of the cochlea, consistent with their being used to extend the high-frequency range. The potential motor role of the short hair cells is an important area for future investigation.

Electromechanical Behavior in Mammalian Outer Hair Cells

The auditory frequency range in submammalian vertebrates rarely exceeds about 5 kHz, but in the evolution of the mammalian hearing organ, this range has been extended by an order of magnitude with the acquisition of new tuning mechanisms. The main morphological innovations are a modification of the middle ear structure, an increase in the length of the basilar membrane, and the specialization of cell types, both supporting and sensory, within the organ of Corti. This specialization includes a separation of the hair cells into two subtypes: a single row of inner hair cells through which most of the auditory information is funneled to the auditory nerve fibers, and three or four rows of long cylindrical outer hair cells with a conspicuous efferent but sparse afferent innervation. Each hair cell type has distinctive response properties (121–123) and makes a differential contribution to the cochlea's sensitivity and frequency selectivity (124). The elongated basilar membrane supports a traveling wave, with a maximum amplitude that moves systematically from apex to base with an increase in stimulation frequency (4). The basilar membrane thus possesses sharp mechanical tuning (125, 126), but as with other frequency-selective mechanisms, the tuning has both passive and active components. The passive component stems mainly from a gradient in the mechanical compliance of the cochlear partition (4). The amplitude of vibration and frequency selectivity are then augmented by active mechanical feedback from the outer hair cells, which generate forces predicted to cancel the viscous damping of the cochlear partition (127, 128).

The current notion of force generation by the outer hair cells involves their contracting longitudinally like miniature muscle fibers (129, 130). The

contractions are fast and voltage-controlled – depolarization inducing cell shortening and hyperpolarization causing elongation. The molecular basis of the mechanism is thought to be a voltage-sensitive motor protein embedded at high densities in the lateral wall of the hair cell (131). Reorientation of the protein in the membrane field, which is envisioned to alter the area per molecule, has been followed by monitoring the associated charge movements (132, 133). Conformational changes in the motor protein are thought to change the surface area of the membrane thus altering the cell length at constant volume. Most of the characterization of outer hair cells has been performed on isolated cells, but in the organ of Corti these cells are constrained by apical attachments to the reticular lamina and by basal connections to Deiters cells. Evidence that outer hair cells can generate sufficient force to deform the organ of Corti is provided by the observation that current passed across the cochlear partition results in basilar membrane movements of tens of nanometers (134).

As with the active hair bundle movements discussed above, the mechanical output frequency is a function of the kinetics of the transducer channels and the speed of the motor. The motor appears to operate up to at least 25 kHz (135) and therefore may not be rate-limiting. However, because the process is voltage-controlled, it is also limited by the membrane time constant, which attenuates the receptor potential at high frequencies. The time constant is the product of the cell capacitance, C , and the input resistance, R , which is dominated by voltage-dependent K^+ conductances. At least two major types of K^+ channel contribute: (a) a high-threshold channel activated at membrane potentials positive to -35 mV and blocked by 0.1 mM 4-aminopyridine; and (b) a low-threshold channel activated between -90 and -50 mV, the identity of which is obscure (136–138). Some evidence also suggests the presence of a Ca^{2+} -activated K^+ channel similar to that found in lower vertebrate hair cells (136, 139).

It is clear that there are cochlear gradients both in the outer hair cell's membrane capacitance (from systematic changes in cell length), and in its complement of K^+ channels. Even the K^+ channel types are differentially expressed, with the high-threshold channel confined to the apical turn of the cochlea and the low-threshold channel predominating in the basal turns (138). Up to a fivefold reduction in cell capacitance from the low- to high-frequency end of the cochlea is accompanied by a severalfold decrease in input resistance (136, 138, 140). Consequently, the cell time constant of high-frequency outer hair cells is an order of magnitude faster than that of low-frequency cells. This is an appropriate trend for minimizing the high-frequency attenuation of the receptor potentials that are required to drive the motor on a cycle by cycle basis. However, absolute values of the time constant have so far yielded equivalent corner frequencies ($F_c = 1/2\pi RC$) of no more than ~ 1 kHz (138, 140, 141). These time constants present a significant rate-limiting step in the electromechanical feedback

loop. The roll-off in sensitivity caused by the membrane time constant may be partially compensated if the magnitude of the transducer current increases in outer hair cells tuned to higher frequencies in mammals as it does in turtle (94).

The contractile behavior of the outer hair cells is a striking mammalian adaptation with properties appropriate for its presumed role as the cochlear amplifier. Owing to its robustness and relative insensitivity to cell metabolism or temperature (142), it has been fairly easy to study. In contrast, elucidating the mechanism and role of active hair bundle movements, which for their manifestation rely on proper functioning of the transduction mechanism, has proved difficult. Nevertheless, it remains a possibility that such bundle movements contribute to mechanical feedback especially at high frequencies. The calcium-dependent feedback described above is likely to be driven by transducer current and therefore is not constrained by the cell membrane time constant. Moreover, the apparent fragility of the hair bundle motor resembles that of the basilar membrane tuning, which is sensitive to the slightest mechanical or metabolic insult to the cochlea and rapidly deteriorates even in the best experimental preparations (e.g. 125). Such vulnerability is most likely located in the mechano-electrical transduction mechanism. The importance of a fully functional transducer in cochlear mechanics is indicated by the effects of treatment with the diuretic furosemide. The main short-term action of furosemide is to reduce the endolymphatic potential, but this results in removal of the sharp tips of both neural and mechanical tuning curves (143, 144). Loss of the endolymphatic potential will reduce the electrical driving force across the stereociliary membrane from 150 to 70 mV, thus roughly halving the transducer current. This argues that the mechanical feedback is strongly sensitive to the gain of the mechano-electrical transduction mechanism. Future experiments should seek to distinguish between the contribution of the transducer and of outer hair cell contractility in generating the active component of basilar membrane tuning.

CONCLUSIONS

The evolution of the auditory receptor is worth summarizing because it may illuminate the limitations of the various mechanisms for frequency selectivity and provide insight into the cellular processes employed in higher vertebrates. The turtle, which has been extensively studied, relies almost exclusively on electrical tuning of the hair cells, perhaps supplemented with active bundle movements driven by a tuned transducer current. The turtle is close to the primitive vertebrate condition, and in more evolutionarily recent amphibians and reptiles there has been an attempt to extend the upper frequency limit by

introduction of various additional mechanisms. An increase in the high-frequency range may stem from selective pressure to improve sound localization in animals with small heads. Frogs possess both a low-frequency amphibian papilla, composed of hair cells endowed with an electrical tuning mechanism, and an organ unique to amphibians that is tuned to the major frequency components of the mating call (1–3 kHz) (145). In lizards, the low-frequency range may also be served by electrical tuning, but in some species the upper frequency limit has been extended to 5 kHz (at room temperature) by use of a secondary papillar region with distinct morphology that utilizes passive mechanical tuning of the hair bundle. These developments would argue that electrical tuning, as described in the turtle, can not be used above about 1 kHz. This may reflect limitations on both the achievable densities and kinetics of the BK channels.

Birds also employ electrical tuning, mediated by either Ca^{2+} -dependent or voltage-activated K^+ channels. The frequency range is partly expanded by elevated temperature, which raises the electrical resonant frequency with a Q_{10} of 2 (146). However, birds also possess other innovations that include a division of labor by inner and outer hair cells and a basilar membrane with some mechanical tuning. The simplest hypothesis is that this mechanical tuning is supplemented by electromechanical feedback from the short (outer) hair cells. Owing to the anchoring of the short hair cells in the basilar papilla, this feedback must be mediated via active hair bundle motion—perhaps transmitted through the tectorial membrane. The upper frequency limit attained is approximately 5 to 10 kHz. The developments found in birds are exaggerated in mammals that utilize a novel electromechanical feedback, by somatic contractions of the outer hair cells, to sharpen the passive mechanical tuning of the basilar membrane. There is no evidence that mammals employ electrical tuning over any frequency range (123, 147), and it may be that the active electromechanical output of the hair bundle also has intrinsic frequency limitations. This question may be settled only by more detailed studies of mammalian cochlear hair cells to investigate their ionic conductances and mechano-electrical transduction mechanism.

ACKNOWLEDGMENTS

Authors' laboratories are supported by NIDCD DC 01362 (RF) and DC 00276, DC 01508 (PF). We thank D Geisler, P Gillespie, M Gray-Keller, G Jones, A Ricci, E Young, and M Zidanic for suggestions on the manuscript, and G Jones and C Dizack for help with the figures.

Visit the *Annual Reviews* home page at
<http://www.AnnualReviews.org>

Literature Cited

1. Musicant AD, Chan JCK, Hind JE. 1990. Direction-dependent spectral properties of cat external ear: new data and cross-species comparisons. *J. Acoust. Soc. Am.* 87:757–81
2. Rice JJ, May BJ, Spirou GA, Young ED. 1992. Pinna-based spectral cues for sound localization in the cat. *Hear. Res.* 58:132–52
3. Webster DB, Fay RR, Popper AN, eds. 1992. *The Evolutionary Biology of Hearing*. New York: Springer-Verlag
4. von Békésy G. 1960. *Experiments in Hearing*, New York: McGraw-Hill
5. Patuzzi R. 1996. Cochlear micromechanics and macromechanics. In *Springer Handbook of Auditory Research. The Cochlea*, ed. P Dallos, AN Popper, RR Fay, 8:186–257. New York: Springer-Verlag
6. Sneary MG. 1988. Auditory receptor of the red-eared turtle: general ultrastructure. *J. Comp. Neurol.* 276:573–87
7. Hackney CM, Fettiplace R, Furness DN. 1993. The functional morphology of stereociliary bundles on turtle cochlear hair cells. *Hear. Res.* 69:163–75
8. O'Neill MP, Bearden A. 1995. Laser feedback measurements of turtle basilar membrane motion using direct reflection. *Hear. Res.* 84:125–38
9. Fettiplace R, Crawford AC. 1978. The coding of sound pressure and frequency in cochlear hair cells of the terrapin. *Proc. R. Soc. London Ser. B* 203:209–18
10. Crawford AC, Fettiplace R. 1980. The frequency selectivity of auditory nerve fibers and hair cells in the cochlea of the turtle. *J. Physiol.* 306:79–125
11. Patterson WC. 1966. Hearing in the turtle. *J. Aud. Res.* 6:453–64
12. Crawford AC, Fettiplace R. 1981. An electrical tuning mechanism in turtle cochlear hair cells. *J. Physiol.* 312:377–412
13. Crawford AC, Fettiplace R. 1983. Auditory nerve responses to imposed displacements of the basilar membrane. *Hear. Res.* 12:199–208
14. Sugihara I, Furukawa T. 1989. Morphological and functional aspects of two different types of hair cells in the goldfish sacculus. *J. Neurophysiol.* 62:1330–43
15. Steinacker A, Romero A. 1992. Voltage-gated potassium current and resonance in toadfish sacculus hair cells. *Brain Res.* 574:229–36
16. Ashmore JF. 1983. Frequency tuning in a frog vestibular organ. *Nature* 304:536–38
17. Lewis RS, Hudspeth AJ. 1983. Voltage- and ion-dependent conductances in solitary vertebrate hair cells. *Nature* 304:538–41
18. Fuchs PA, Evans MG. 1988. Voltage oscillations and ionic conductances in hair cells isolated from the alligator cochlea. *J. Comp. Physiol.* 164:151–63
19. Fuchs PA, Nagai T, Evans MG. 1988. Electrical tuning in hair cells isolated from the chick cochlea. *J. Neurosci.* 8:2460–67
20. Hudspeth AJ, Lewis RS. 1988. Kinetic analysis of voltage- and ion-dependent conductances in saccular hair cells of the bullfrog, *Rana catesbeiana*. *J. Physiol.* 400:237–74
21. Hudspeth AJ, Lewis RS. 1988. A model for electrical resonance and frequency tuning in saccular hair cells of the bullfrog, *Rana catesbeiana*. *J. Physiol.* 400:275–97
22. Art JJ, Fettiplace R. 1987. Variation of membrane properties in hair cells isolated from the turtle cochlea. *J. Physiol.* 385:207–42
23. Art JJ, Wu YC, Fettiplace R. 1995. The calcium-activated potassium channels of turtle hair cells. *J. Gen. Physiol.* 105:49–72
24. Wu YC, Art JJ, Goodman MB, Fettiplace R. 1995. A kinetic description of the calcium-activated potassium channel and its application to electrical tuning of hair cells. *Prog. Biophys. Mol. Biol.* 63:131–58
25. Ohmori H. 1984. Studies of ionic currents in the isolated vestibular hair cell of the chick. *J. Physiol.* 350:561–81
26. Fuchs PA, Evans MG, Murrow BW. 1990. Calcium current in hair cells isolated from the cochlea of the chick. *J. Physiol.* 429:553–68
27. Roberts WM, Jacobs RA, Hudspeth AJ. 1990. Co-localization of ion channels involved in frequency selectivity and synaptic transmission at presynaptic active zones of hair cells. *J. Neurosci.* 10:3664–84
28. Prigioni I, Masetto S, Russo G, Taglietti V. 1992. Calcium currents in solitary hair cells isolated from frog crista ampullaris. *J. Vestibular Res.* 2:31–9
29. Zidanic M, Fuchs PA. 1995. Kinetic analysis of barium currents in chick cochlear hair cells. *Biophys. J.* 68:1323–36
30. Kollmar R, Montgomery LG, Fak J,

- Henry LJ, Hudspeth AJ. 1998. Predominance of the α_{1D} subunit in L-type voltage-gated Ca^{2+} channels of hair cells in the chicken's cochlea. *Proc. Natl. Acad. Sci. USA* 94:14883–88
31. Art JJ, Fettiplace R, Wu Y-C. 1993. The effects of low calcium on the voltage-dependent conductances involved in the tuning of turtle hair cells. *J. Physiol.* 470:109–26
 32. Wu Y-C, Fettiplace R. 1996. A developmental model for generating frequency maps in the reptilian and avian cochleas. *Biophys. J.* 70:2557–70
 33. Atkinson NS, Robertson GA, Ganetzky B. 1991. A component of calcium-activated potassium channels encoded by the *Drosophila slo* locus. *Science* 253:551–55
 34. Adelman JP, Shen K-Z, Kavanaugh MP, Warren RA, Wu Y-N, et al. 1992. Calcium-activated potassium channels expressed from cloned complementary DNAs. *Neuron* 9:209–16
 35. Butler A, Tsunoda S, McCobb DP, Wei A, Salkoff L. 1993. *mslo*, a complex mouse gene encoding “maxi” calcium-activated potassium channels. *Science* 261:221–24
 36. Tseng-Crank J, Foster CD, Krause JD, Mertz R, Godinot N, et al. 1994. Cloning, expression and distribution of functionally distinct Ca^{2+} -activated K^+ channel isoforms from human brain. *Neuron* 13:1315–30
 37. McCobb DP, Fowler NL, Featherstone T, Lingle CJ, Saito M, et al. 1995. A human calcium-activated potassium channel gene expressed in vascular smooth muscle. *Am. J. Physiol.* 269:H767–77
 38. Jiang G-J, Židanic M, Michaels R, Michael T, Griguer C, Fuchs PA. 1997. *cslo* encodes Ca^{2+} -activated potassium channels in the chick's cochlea. *Proc. R. Soc. London Ser. B* 264:731–37
 39. Jones EMC, Laus C, Fettiplace R. 1998. Identification of Ca^{2+} -activated K^+ channel splice variants and their distribution in the turtle cochlea. *Proc. R. Soc. London Ser. B* 265:685–92
 40. Navaratnam DS, Bell TJ, Tu TD, Cohen EL, Oberholtzer JC. 1997. Differential distribution of Ca^{2+} -activated K^+ channel splice variants among hair cells along the tonotopic axis of the chick cochlea. *Neuron* 19:1077–85
 41. Rosenblatt KP, Sun Z-P, Heller S, Hudspeth AJ. 1997. Distribution of Ca^{2+} -activated K^+ channel isoforms along the tonotopic gradient of the chicken's cochlea. *Neuron* 19:1061–75
 42. Meera P, Wallner M, Song M, Toro L. 1997. Large conductance voltage- and Ca^{2+} -activated K^+ channel, a distinct member of voltage-dependent ion channels with seven N-terminal transmembrane segments (S0–S6), an extracellular N-terminus and an intracellular (S9–S10) C-terminus. *Proc. Natl. Acad. Sci. USA* 94:14066–71
 43. Wei A, Solaro C, Lingle C, Salkoff L. 1994. Calcium sensitivity of BK-type K_{Ca} channels determined by a separable domain. *Neuron* 13:671–81
 44. Lagrutta A, Shen K-Z, North RA, Adelman JP. 1994. Functional differences among alternatively spliced variants of Slowpoke, a *Drosophila* calcium-activated potassium channel. *J. Biol. Chem.* 269:20347–51
 45. Saito M, Nelson C, Salkoff L, Lingle CJ. 1997. A cysteine-rich domain defined by a novel exon in a *slo* variant in rat adrenal chromaffin cells and PC12 cells. *J. Biol. Chem.* 272:11710–17
 46. Michael T, Ramanathan K, Jones EMC, Art JJ, Fettiplace R, Fuchs PA. 1997. Functional expression of cochlear Slo potassium channels in HEK293 cells and *Xenopus* oocytes. *Biophys. J.* 72:A352 (Abstr.)
 47. Xie J, McCobb DP. 1998. Control of alternative splicing of potassium channels by stress hormones. *Science* 280:443–46
 48. Michael T, Jiang G-J, Ramanathan K, Fuchs PA. 1998. BK channels encoded by cSlo splice variants from the chick's cochlea. *Assoc. Res. Otolaryngol.* 21:82 (Abstr.)
 49. Jones EMC, Gray-Keller M, Art JJ, Fettiplace R. 1998. The functional role of alternative splicing of Ca^{2+} -activated K^+ channels in auditory hair cells. In *Molecular and Functional Diversity of Ion Channels and Receptors*, ed. B Rudy, P Seeburg. New York: Ann. NY Acad. Sci. In press
 50. McManus OB, Helms LM, Pallanck L, Ganetzky B, Swanson R, Leonard RJ. 1995. Functional role of β -subunit of high-conductance calcium-activated potassium channels. *Neuron* 14:645–50
 51. Ramanathan K, Michael T, Jiang G-J, Hiel H, Fuchs PA. 1998. A molecular mechanism for electrical tuning of cochlear hair cells. *Science*. In press
 52. Fuchs PA, Evans MG. 1990. Potassium currents in hair cells isolated from the cochlea of the chick. *J. Physiol.* 429:529–51
 53. Evans MG, Fuchs PA. 1987. Tetrodotoxin-sensitive voltage-dependent sodi-

- um currents in hair cells from the alligator cochlea. *Biophys. J.* 52:649–52
54. Goodman M, Art JJ. 1996. Variations in the ensemble of potassium currents underlying resonance in turtle hair cells. *J. Physiol.* 497:395–412
 55. Goodman M, Art JJ. 1996. Positive feedback by a potassium selective inward rectifier enhances tuning in vertebrate hair cells. *Biophys. J.* 71:430–42
 56. Navaratnam DS, Escobar L, Covarrubias M, Oberholtzer JC. 1995. Permeation properties and differential expression across the auditory receptor epithelium of an inward rectifier K^+ channel cloned from the chick inner ear. *J. Biol. Chem.* 270:19238–45
 57. Issa N, Hudspeth AJ. 1994. Clustering of Ca^{2+} channels and Ca^{2+} -activated K^+ channels at fluorescently labeled presynaptic active zones of hair cells. *Proc. Natl. Acad. Sci. USA* 91:7578–82
 58. Robitaille R, Charlton MP. 1992. Presynaptic calcium signals and transmitter release are modulated by calcium-activated potassium channels. *J. Neurosci.* 12:297–305
 59. Martinez-Dunst C, Michaels RL, Fuchs PA. 1997. Release sites and calcium channels in hair cells of the chick's cochlea. *J. Neurosci.* 17:9133–44
 60. Sneary MG. 1988. Auditory receptor of the red-eared turtle. II. Afferent and efferent synapses and innervation patterns. *J. Comp. Neurol.* 276:588–606
 61. Fischer F. 1992. Quantitative analysis of the innervation pattern of the chicken basilar papilla. *Hear. Res.* 61:167–78
 62. Murrow BW. 1994. Position-dependent expression of potassium currents by hair cells of the chick's cochlea. *J. Physiol.* 480:247–59
 63. Sheng M, Tsaur M-L, Jan YN, Jan LY. 1992. Subcellular segregation of two A-type K^+ channel proteins in rat central neurons. *Neuron* 9:271–84
 64. Sokolowski BHA, Stahl L, Fuchs PA. 1993. Morphological and physiological development of vestibular hair cells in the organ-cultured otocyst of the chick. *Dev. Biol.* 155:134–46
 65. Hirokawa N. 1977. Disappearance of afferent and efferent nerve terminals in the inner ear of the chick embryo after chronic treatment with beta-bungarotoxin. *J. Cell. Biol.* 73:27–46
 66. Fuchs PA, Sokolowski BHA. 1990. The acquisition during development of Ca -activated potassium currents by cochlear hair cells of the chick. *Proc. R. Soc. London Ser. B* 241:122–26
 67. Saunders JC, Coles RB, Gates GR. 1973. The development of auditory evoked responses in the cochlea and cochlear nuclei of the chick. *Brain Res.* 63:59–74
 68. Jones SM, Jones TA. 1995. The tonotopic map in the embryonic chicken cochlea. *Hear. Res.* 82:149–57
 69. Griguer C, Fuchs PA. 1996. Voltage-dependent potassium currents in cochlear hair cells of the embryonic chick. *J. Neurophysiol.* 75:508–13
 70. Gu X, Spitzer NC. 1995. Distinct aspects of neuronal differentiation encoded by frequency of spontaneous Ca^{2+} transients. *Nature* 375:784–87
 71. Hudspeth AJ. 1982. Extracellular current flow and the site of transduction by vertebrate hair cells. *J. Neurosci.* 2:1–10
 72. Jaramillo F, Hudspeth AJ. 1992. Localization of the hair cell's transduction channels at the hair bundle's top by iontophoretic application of a channel blocker. *Neuron* 7:409–20
 73. Denk W, Holt JR, Shepherd GMG, Corey DP. 1995. Calcium imaging of single stereocilia in hair cells: localization of transduction channels at both ends of tip links. *Neuron* 15:1311–21
 74. Pickles JO, Comis SD, Osborne MP. 1984. Crosslinks between the stereocilia in the guinea pig organ of Corti, and the possible relation to sensory transduction. *Hear. Res.* 15:103–12
 75. Assad JA, Shepherd GMG, Corey DP. 1991. Tip-link integrity and mechanical transduction in a vertebrate hair cell. *Neuron* 7:985–94
 76. Mulroy MJ. 1974. Cochlear anatomy of the alligator lizard. *Brain Behav. Evol.* 10:69–87
 77. Lim DJ. 1980. Cochlear anatomy related to cochlear micromechanics: a review. *J. Acoust. Soc. Am.* 67:1686–95
 78. Turner RG, Muraski AA, Nielsen DW. 1981. Cilium length influences on tonotopic organization. *Science* 213:1519–21
 79. Tilney LG, Saunders JC. 1983. Actin filaments, stereocilia and hair cells of the bird cochlea. I. Length, width and distribution of stereocilia of each hair cell are related to the position of the hair cell on the cochlea. *J. Cell Biol.* 96:807–21
 80. Köppl C, Authier S. 1995. Quantitative anatomical basis for a model of micromechanical tuning in the Tokay gecko, (*Gekko gekko*). *Hear. Res.* 82:14–25
 81. Flock A, Flock B, Murray E. 1977. Studies on the sensory hairs of receptor cells in the inner ear. *Acta Otolaryngol.* 83:85–91

82. Crawford AC, Fettiplace R. 1985. The mechanical properties of ciliary bundles of turtle cochlear hair cells. *J. Physiol.* 364:359-79
83. Howard J, Ashmore JF. 1986. Stiffness of sensory hair bundles in the sacculus of the frog. *Hear. Res.* 23:93-104
84. Pickles JO. 1993. A model for the mechanics of the stereociliar bundle on acousticolateral hair cells. *Hear. Res.* 68: 159-72
85. Weiss TF, Leong R. 1985. A model for signal transmission in an ear having hair cells with free-standing stereocilia. III. Micromechanical stage. *Hear. Res.* 20:157-74
86. Strelieff D, Flock A, Minser KE. 1985. Role of inner and outer hair cells in mechanical frequency selectivity of the cochlea. *Hear. Res.* 18:169-75
87. Wever EG. 1978. *The Reptile Ear: Its Structure and Function*. Princeton, NJ: Princeton Univ. Press
88. Freeman DM, Weiss TF. 1990. Hydrodynamic analysis of a two-dimensional model for micromechanical resonance of free-standing hair bundles. *Hear. Res.* 48: 37-68
89. Frishkopf LS, DeRosier DJ. 1983. Mechanical tuning of free-standing stereociliary bundles and frequency analysis in the alligator lizard cochlea. *Hear. Res.* 12: 393-404
90. Holton T, Hudspeth AJ. 1983. A micromechanical contribution to cochlear tuning and tonotopic organization. *Science* 222:508-10
91. Manley GA, Yates GK, Köppl C. 1988. Auditory peripheral tuning: evidence for a simple resonance phenomenon in the lizard *Tiliqua*. *Hear. Res.* 181-90
92. Authier S, Manley GA. 1995. A model of frequency tuning in the basilar papilla of the Tokay gecko, *Gekko gekko*. *Hear. Res.* 82:1-13
93. Eatock RA, Manley GA, Pawson L. 1981. Auditory nerve fibre activity in the Tokay gecko: implications for cochlear processing. *J. Comp. Physiol.* 142:203-18
94. Ricci AJ, Fettiplace R. 1997. The effects of calcium buffering and cyclic AMP on mechano-electrical transduction in turtle auditory hair cells. *J. Physiol.* 501:111-24
95. Corey DP, Hudspeth AJ. 1983. Analysis of the microphonic potentials of the bullfrog sacculus. *J. Neurosci.* 3:942-61
96. Eatock RA, Corey DP, Hudspeth AJ. 1987. Adaptation of mechano-electrical transduction in hair cells of the bullfrog's sacculus. *J. Neurosci.* 7:2821-36
97. Ohmori H. 1985. Mechano-electrical transduction currents in isolated vestibular hair cells of the chick. *J. Physiol.* 359:189-217
98. Assad JA, Hacohen N, Corey DP. 1989. Voltage dependence of adaptation and active bundle movements in bullfrog sacculus hair cells. *Proc. Natl. Acad. Sci. USA* 86:2918-22
99. Crawford AC, Evans MG, Fettiplace R. 1989. Activation and adaptation of transducer currents in turtle hair cells. *J. Physiol.* 419:405-34
100. Crawford AC, Evans MG, Fettiplace R. 1991. The actions of calcium on the mechano-electrical transducer current of turtle hair cells. *J. Physiol.* 434:369-98
101. Assad JA, Corey DP. 1992. An active motor model for adaptation by vertebrate hair cells. *J. Neurosci.* 12:3291-309
102. Kros CJ, Rüsch A, Richardson GP. 1992. Mechano-electrical transducer currents in hair cells of the cultured neonatal mouse. *Proc. R. Soc. London Ser. B* 249:185-93
103. Art JJ, Fettiplace R. 1984. Efferent desensitization of auditory nerve fibre responses in the cochlea of the turtle *Pseudemys scripta elegans*. *J. Physiol.* 356:507-23
104. Ricci AJ, Wu Y-C, Fettiplace R. 1998. The endogenous calcium buffer and the time course of transducer adaptation in turtle auditory hair cells. *J. Neurosci.* 18: 8261-77
105. Ricci AJ, Fettiplace R. 1998. Calcium permeation of the turtle hair cell's mechano-transducer channel and its relation to the composition of endolymph. *J. Physiol.* 506:159-73
106. Hudspeth AJ, Gillespie PG. 1994. Pulling strings to tune transduction. Adaptation by hair cells. *Neuron* 12:1-9
107. Hasson T, Gillespie PG, Garcia JA, MacDonald RB, Zhao Y, et al. 1997. Unconventional myosins in inner-ear sensory epithelia. *J. Cell Biol.* 137:1287-307
108. Gillespie PG, Hudspeth AJ. 1993. Adenine nucleoside diphosphates block adaptation of mechano-electrical transduction in hair cells. *Proc. Natl. Acad. Sci. USA* 90:2710-14
109. Yamoah EN, Gillespie PG. 1996. Phosphate analogs block adaptation by inhibiting adaptation-motor force production. *Neuron* 17:523-33
110. Tucker T, Fettiplace R. 1995. Confocal imaging of calcium microdomains and calcium extrusion in turtle hair cells. *Neuron* 15:1323-35

111. Yamoah EN, Lumpkin EA, Dumont RA, Smith PJS, Hudspeth AJ, Gillespie PG. 1998. Plasma membrane Ca^{2+} -ATPase extrudes Ca^{2+} from hair cell stereocilia. *J. Neurosci.* 18:610–24
112. Howard J, Hudspeth AJ. 1987. Mechanical relaxation of the hair bundle mediates adaptation in mechano-electrical transduction by the bullfrog's saccular hair cell. *Proc. Natl. Acad. Sci. USA* 84:3064–68
113. Rüsçh A, Thurm U. 1990. Spontaneous and electrically induced movements of ampullary kinocilia and stereovilli. *Hear. Res.* 48:247–64
114. Denk W, Webb WW. 1993. Forward and reverse transduction at the limit of sensitivity studied by correlating electrical and mechanical fluctuations in frog saccular hair cells. *Hear. Res.* 60:89–102
115. Benser ME, Marquis RE, Hudspeth AJ. 1996. Rapid, active hair bundle movements in hair cells from the bullfrog's sacculus. *J. Neurosci.* 16:5629–43
116. Brix J, Manley GA. 1994. Mechanical and electromechanical properties of the stereovillar bundles of isolated and cultured hair cells of the chicken. *Hear. Res.* 76:147–57
117. Manley GA, Gallo L. 1997. Otoacoustic emissions, hair cells and myosin motors. *J. Acoust. Soc. Am.* 102:1049–55
118. Köppl C. 1995. Otoacoustic emissions as an indicator for active cochlear mechanics: a primitive property of vertebrate auditory organs. In *Advances in Hearing Research* ed. GA Manley, GM Klump, C Köppl, H Fastl, H Oeckinghaus, pp. 207–16. Singapore: World Sci.
119. Tanaka K, Smith CA. 1978. Structure of the chicken's inner ear: SEM and TEM study. *Am. J. Anat.* 153:251–72
120. Gummer AW, Smolders JWT, Klinke R. 1987. Basilar membrane motion in the pigeon measured with the Mössbauer technique. *Hear. Res.* 29:63–92
121. Dallos P. 1985. Response characteristics of mammalian cochlear hair cells. *J. Neurosci.* 5:1591–608
122. Russell IJ, Cody AR, Richardson GP. 1986. The responses of inner and outer hair cells in the basal turn of the guinea-pig cochlea and in the mouse cochlea grown in vitro. *Hear. Res.* 22:199–216
123. Kros CJ. 1996. Physiology of mammalian cochlear hair cells. In *Springer Handbook of Auditory Research: The Cochlea*, ed. P Dallos, AN Popper, RR Fay. 8:318–85. New York: Springer-Verlag
124. Kiang NYS, Liberman MC, Sewell WF, Guinan JJ. 1986. Single unit clues to cochlear mechanisms. *Hear. Res.* 22:171–82
125. Rhode WS. 1971. Observations on the vibrations of the basilar membrane in squirrel monkeys using the Mössbauer technique. *J. Acoust. Soc. Am.* 49:1218–31
126. Patuzzi R, Robertson D. 1988. Tuning in the mammalian cochlea. *Physiol. Rev.* 68:1009–82
127. de Boer E. 1983. No sharpening? A challenge for cochlear mechanics. *J. Acoust. Soc. Am.* 73:567–73
128. Neely ST, Kim DO. 1983. An active cochlear model shows sharp tuning and high sensitivity. *Hear. Res.* 9:123–30
129. Brownell WE, Bader CR, Bertrand D, de Ribaupierre Y. 1985. Evoked mechanical responses of isolated cochlear outer hair cells. *Science* 227:194–96
130. Ashmore JF. 1987. A fast motile response in guinea-pig outer hair cells: the cellular basis for the cochlear amplifier. *J. Physiol.* 388:323–47
131. Kalinec F, Holley MC, Iwasa KH, Lim DJ, Kachar BA. 1992. A membrane-based force generation mechanism in auditory sensory cells. *Proc. Natl. Acad. Sci. USA* 89:8671–75
132. Santos-Sacchi J. 1991. Reversible inhibition of voltage-dependent outer hair cell motility and capacitance. *J. Neurosci.* 11:3096–110
133. Tunstall MJ, Gale JE, Ashmore JF. 1995. Action of salicylate on membrane capacitance of outer hair cells from the guinea-pig cochlea. *J. Physiol.* 485:739–52
134. Mammano F, Ashmore JF. 1993. Reverse transduction measured in the isolated cochlea by laser Michelson interferometry. *Nature* 365:838–41
135. Gale JE, Ashmore JF. 1997. An intrinsic frequency limit to the cochlear amplifier. *Nature* 389:63–66
136. Housley GD, Ashmore JF. 1992. Ionic currents of outer hair cells isolated from the guinea-pig cochlea. *J. Physiol.* 448:73–98
137. Nakagawa T, Kakehata S, Yamamoto T, Akaïke N, Komune S, Uemura T. 1994. Ionic properties of $I_{K,n}$ in outer hair cells of guinea pig cochlea. *Brain Res.* 661:293–97
138. Mammano F, Ashmore JF. 1996. Differential expression of outer hair cell potassium currents in the isolated cochlea of the guinea pig. *J. Physiol.* 496:639–46
139. Nenov AP, Norris C, Bobbin RP. 1997. Outwardly rectifying currents in guinea

- pig outer hair cells. *Hear. Res.* 105:146–58
140. Preyer P, Renz S, Hemmert W, Zenner H-P, Gummer AW. 1996. Receptor potential of outer hair cells isolated from base to apex of the adult guinea-pig cochlea: implications for cochlear tuning mechanisms. *Aud. Neurosci.* 2:145–57
 141. Santos-Sacchi J. 1992. On the frequency limit and phase of outer hair cell motility: effects of the membrane filter. *J. Neurosci.* 12:1906–16
 142. Holley MC, Ashmore JF. 1988. On the mechanism of a high-frequency force generator in outer hair cells isolated from the guinea-pig cochlea. *Proc. R. Soc. London Ser. B* 232:413–29
 143. Sewell WF. 1984. The effect of furosemide on the endocochlear potential and auditory nerve fiber tuning curves in cats. *Hear. Res.* 14:305–14
 144. Ruggero MA, Rich NC. 1991. Furosemide alters organ of Corti mechanics: evidence for feedback of outer hair cells upon basilar membrane. *J. Neurosci.* 11:1057–67
 145. Zakon HH, Wilczynski W. 1988. The physiology of the anuran eighth nerve. In *The Evolution of the Amphibian Auditory System*, ed. B Fritzsche, MJ Ryan, W Wilczynski, TE Hetherington, W Walkowiak, pp. 125–55. New York: Wiley
 146. Schermuly L, Klinke R. 1985. Changes of characteristic frequency of pigeon primary afferents with temperature. *J. Comp. Physiol. A* 156:209–11
 147. Kros CJ, Crawford AC. 1990. Potassium currents in inner hair cells isolated from the guinea-pig cochlea. *J. Physiol.* 421:263–92
 148. Wallner M, Meera P, Toro L. 1996. Determinant for β -subunit regulation in high-conductance voltage-activated and Ca^{2+} -sensitive K^+ channels: an additional transmembrane region at the N-terminus. *Proc. Natl. Acad. Sci. USA* 93:14922–27



CONTENTS

Pulling the Cart and Enjoying the Ride, <i>Carlton C. Hunt</i>	1
Cellular and Molecular Basis for Electrical Rhythmicity in Gastrointestinal Muscles, <i>Burton Horowitz, Sean M. Ward, Kenton M. Sanders</i>	19
Ionic Conductances in Gastrointestinal Smooth Muscles and Interstitial Cells of Cajal, <i>G. Farrugia</i>	45
Excitation-Contraction Coupling in Gastrointestinal and Other Smooth Muscles, <i>T. B. Bolton, S. A. Prestwich, A. V. Zholos, D. V. Gordienko</i>	85
THE ENTERIC NERVOUS SYSTEM AND REGULATION OF INTESTINAL MOTILITY, <i>W. A. A. Kunze, J. B. Furness</i>	117
Mechanisms of Cardiac Pain, <i>R. D. Foreman</i>	143
Desensitization of G Protein-Coupled Receptors in the Cardiovascular System, <i>M. Bünemann, K. B. Lee, R. Pals-Rylandsdam, A. G. Roseberry, M. M. Hosey</i>	169
Regulation of Natriuretic Peptide Secretion by the Heart, <i>G. Thibault, F. Amiri, R. Garcia</i>	193
Myoblast Cell Grafting into Heart Muscle: Cellular Biology and Potential Applications, <i>P. D. Kessler, B. J. Byrne</i>	219
Heat-Shock Proteins, Molecular Chaperones, and the Stress Response: Evolutionary and Ecological Physiology, <i>Martin E. Feder, Gretchen E. Hofmann</i>	243
Genetic Diseases and Gene Knockouts Reveal Diverse Connexin Functions, <i>Thomas W. White, David L. Paul</i>	283
Localized Intracellular Calcium Signaling in Muscle: Calcium Sparks and Calcium Quarks, <i>Ernst Niggli</i>	311
ATP-Sensitive Potassium Channels: A Model of Heteromultimeric Potassium Channel/Receptor Assemblies, <i>Susumu Seino</i>	337
Adrenomedullin and the Control of Fluid and Electrolyte Homeostasis, <i>Willis K. Samson</i>	363
Pathophysiology of Endothelin in the Cardiovascular System, <i>Takashi Miyachi, Tomoh Masaki</i>	391
Gene Interactions in Gonadal Development, <i>Keith L. Parker, Andreas Schedl, Bernard P. Schimmer</i>	417
Synchronous Activity in the Visual System, <i>W. Martin Usrey, R. Clay Reid</i>	435
Timing in the Auditory System of the Bat, <i>Ellen Covey, John H. Casseday</i>	457
Synaptic Mechanisms for Coding Timing in Auditory Neurons, <i>Laurence O. Trussell</i>	477
The Role of Timing in the Brainstem Auditory Nuclei of Vertebrates, <i>D. Oertel</i>	497
TIMING OF SYNAPTIC TRANSMISSION, <i>B. L. Sabatini, W. G. Regehr</i>	521
Structure, Strength, Failure, and Remodeling of the Pulmonary Blood-Gas Barrier, <i>J. B. West, O. Mathieu-Costello</i>	543
Evolution of Vertebrate Cardio-Pulmonary System, <i>C. G. Farmer</i>	573

Mouse Models of Airway Responsiveness: Physiological Basis of Observed Outcomes and Analysis of Selected Examples Using These Outcome Indicators, <i>J. M. Drazen, P. W. Finn, G. T. De Sanctis</i>	593
Sodium Channels in Alveolar Epithelial Cells: Molecular Characterization, Biophysical Properties, and Physiological Significance, <i>Sadis Matalon, Hugh O'Brodovich</i>	627
Sodium-Coupled Transporters for Krebs Cycle Intermediates, <i>Ana M. Pajor</i>	663
Modulation of Vasopressin-Elicited Water Transport by Trafficking of Aquaporin2-Containing Vesicles, <i>Donald T. Ward, Timothy G. Hammond, H. William Harris</i>	683
Electrogenic Na ⁺ /HCO ₃ ⁻ Cotransporters: Cloning and Physiology, <i>Michael F. Romero, Walter F. Boron</i>	699
Electrophysiology of Synaptic Vesicle Cycling, <i>Henrique von Gersdorff, Gary Matthews</i>	725
Genetics of Synaptic Vesicle Function: Toward the Complete Functional Anatomy of an Organelle, <i>Rafael Fernández-Chacón, Thomas C. Südhof</i>	753
RECONSTITUTION OF REGULATED EXOCYTOSIS IN CELL-FREE SYSTEMS: A Critical Appraisal, <i>Julia Avery, Reinhard Jahn, J. Michael Edwardson</i>	777
Mechanisms of Hair Cell Tuning, <i>R. Fettiplace, P. A. Fuchs</i>	809
Ion Channels of Nociception, <i>Edwin W. McCleskey, Michael S. Gold</i>	835
Controversial Issues in Vertebrate Olfactory Transduction, <i>Geoffrey H. Gold</i>	857
Cellular Mechanisms of Taste Transduction, <i>M. Scott Herness, Timothy A. Gilbertson</i>	873